REVISTA MATÉRIA V.29 N.1
ISSN 1517-7076 articles e20230335, 2024

Utilizing binary ternary blended metakaolin and ground pond ash for reduced carbon footprint emissions and improved mechanical properties in concrete

Yuvaraj Kandasamy[1], Vidhya Kumarasamy[2], Sakthivel Murugan[3], Ramkumar Singaraj[4]

[1]K.S. Rangasamy College of Technology, Department of Civil Engineering. Tiruchengode, 637 215, Namakkal, Tamilnadu, India.

[2]Mahendra Engineering College, Department of Civil Engineering. Tiruchengode, 637 501, Namakkal, Tamilnadu, India.

[3]Kongunadu College of Engineering and Technology, Department of Civil Engineering. Tholurpatti, 621 215, Trichy, Tamilnadu, India.

[4]K. Ramakrishnan College of Technology, Department of Civil Engineering. Samayapuram, 621 112, Trichy, Tamilnadu, India.

e-mail: yuva02raj@gmail.com, vidhya22047@gmail.com, aries.sakthi@gmail.com, ramsvgrcivil@gmail.com

ABSTRACT

In this empirical investigation, the effect of four concrete mixtures was examined, namely, control concrete (CC), binary blended metakaolin concrete (BBMC), binary blended pond ash concrete (BBPC), and ternary blended metakaolin and pond ash concrete (TBMPC). In this study, a total of 288 specimens were manufactured, including CC, BBMC, BBPC, and TBMPC, which were subjected to curing for 28 and 90 days. The mix compositions used were in a ratio of 1:1.75:2.22, with a water-binder ratio of 0.44. The study delved into an extensive examination of both the fresh and mechanical properties of these concrete mixtures. Additionally, the sustainability analysis for all mix proportions were computed. The results demonstrate significant enhancements in compressive strength (f_{cs}), split tensile strength (f_{sts}) and flexural strength (f_{fs}) with an increase of 17.82% and 19.81%, 12.32% and 13.50%, 13.34% and 14.39%. These improvements were observed specifically in the M_6P_6 mix, composed of 88% PC, 6% MK, and 6% PA. In the context of sustainability analysis, the PA_{20} mix displayed the lowest carbon footprint emissions, measured at 351 $kgCO_2/m^3$. On the other hand, the MK_6PA_6 mix demonstrated the highest CO_2 intensity, with values of 0.095 $MPa/kgCO_2 \cdot m^3$ and 0.114 $MPa/kgCO_2 \cdot m^3$.

Keywords: Metakaolin; Pond ash; Fresh properties; Mechanical properties; Carbon footprint emissions.

1. INTRODUCTION

Globally, concrete plays a pivotal role and most extensively utilized construction material. It excels as the superior construction material when contrasted with alternatives like brick, wood, steel, and others [1]. The widespread use of concrete has adverse effects on the ecosystem. This is primarily attributed to the presence of cement in concrete, leading to the release of substantial amounts of carbon emissions. In India, the cement sector is projected to generate approximately 390 MTPA by the end of 2023. Anticipated growth in Indian cement demand for 2024 suggests an increase of around 9%, bringing it to 425 MT [2]. According to NAQI and JANG [3], nearly half of the global cement production is dedicated to serving the concrete production industry, while the remaining portion finds application in various uses, including masonry mortar and filling cracks in concrete elements. A noteworthy observation that with the escalating demand and the anticipated growth in cement production in the years ahead, it becomes imperative to explore alternative materials that can effectively substitute cement. This strategic shift is a critical measure in the endeavor to mitigate CO_2 emissions [4, 5]. Conversely, there exists an immense global waste output, amounting to millions of tons, which holds the potential for recycling as a binder or aggregate element within concrete. This endeavor aims to curtail the carbon footprint of concrete production [6]. These waste materials encompass industrial byproducts [7–11] and agricultural byproducts [12–16].

Metakaolin (MK) is a pozzolan obtained from kaolin, created through a process involving the heating clay rich in kaolinite to temperatures ranging from 500 °C to 800 °C [17]. MK is composed of varying proportions of alumina and silica, typically in the ranges of 40% to 45% for alumina and 50% to 55% for silica.

Corresponding Author: Yuvaraj Kandasamy Received on 27/11/2023 Accepted on 22/01/2024

DOI: https://doi.org/10.1590/1517-7076-RMAT-2023-0335

Typically, it presents as a colorless powder with an average size of 2 μm diameter, making it significantly finer than particles in cement [18]. MK is widely recognized for its positive impact on enhancing the efficacy of concrete. This improvement is achieved through its reaction with existing portlandite to create secondary formation of calcium silicate hydrate gel and several other hydrates gel [19]. This observation has also been documented in [20–23]. Consequently, utilizing metakaolin is a more cost-effective choice compared to using silica fume [24]. Most studies that have investigated the use of MK as a pozzolan in concrete have shown significant improvements when used as a replacement [25–27]. The incorporation of 15% MK leads to significant improvements in concrete [28].

Moreover, the majority of research on the utilization of pond ash (PA) has primarily centered on its application as fine aggregates in concrete, mainly because of its coarser texture [29–32]. Nevertheless, to achieve more substantial reductions in the carbon footprint of concrete, a greater emphasis should be placed on replacing cement, which stands out as the component with the highest carbon footprint in concrete production [33]. Consequently, the process involves pulverizing PA through the use of a pulverizer machine to yield a finer product, known as finer PA, distinguished by its high silicate and aluminate content [34, 35]. As a result, the transformation of coarser PA into finer PA and its subsequent incorporation as a pozzolan is anticipated to lead to an overall reduction in the environmental impact of concrete [36, 37]. Based on the KURAMA and KAYA [38] findings, it was deduced that incorporating PA as a replacement material for cement, up to a 10% dosage, can enhance the concrete attributes. Consequently, it holds potential for utilization in the concrete sector.

Ternary blended concrete (TBC), whether incorporating MK with fly ash [39], MK with silica fume [40], MK with rice husk ash [41], MK with GGBS [42], MK with sugarcane bagasse ash [43], MK with Alccofine [44], MK with Nano silica [45], MK with dolomite powder [46], demonstrates enhanced mechanical properties and decreased porosity. Notably, the reduction in pore spaces in TBC becomes more pronounced with increasing dosages of pozzolans after 28 days.

In the existing body of research, the majority of scholars have directed their investigations towards the effects of binary blended metakaolin concrete (BBMC) and binary blended pond ash concrete (BBPC). Surprisingly, there has been a notable absence of investigation into the ternary blended metakaolin and pond ash concrete (TBMPC). As a result, the primary goal of this research endeavor is to investigate the impact and carbon footprint of BBMC, BBPC, and TBMPC mixtures.

2. MATERIALS AND EXPERIMENTAL PROGRAM

2.1. Materials

Pond ash (PA) was collected from Mettur, Tamil Nadu, India, was air-dried for 48 hours. It was then sifted through a 300-micron sieve to eliminate larger particles and finely ground with a pulverizer operating at 960 rpm. Meanwhile, metakaolin (MK) is a naturally occurring pozzolanic material sourced from Chennai, Tamil Nadu, India. Additionally, 53-grade Portland cement (PC) was purchased from a local supplier, meeting the BIS 12269–2013 [47]. Figures 1 and 2 depict the scanning electron microscope (SEM) images of MK and PA, respectively.

In Figure 1, illustrates angular, and platy particle structure. In Figure 2, on the other hand, the spherical structure of PA has been disrupted and transformed into angular, fragmented particles. The PC served as the

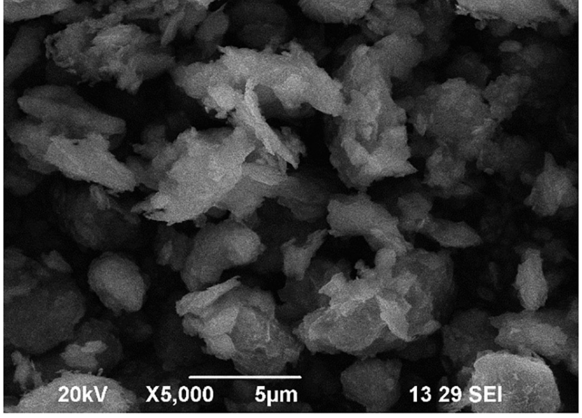

Figure 1: SEM image of MK.

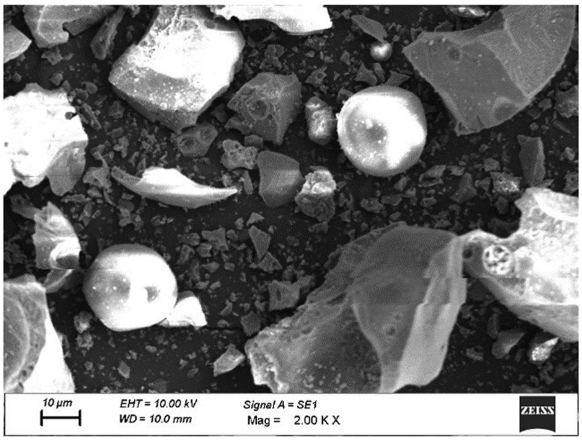

Figure 2: SEM image of PA.

Table 1: Physical properties and oxide composition of PC, MK and PA.

ELEMENTS	OXIDES (%)		
	PC	MK	PA
SiO_2	21.9	50.11	51.4
Al_2O_3	5.63	43.08	29.2
Fe_2O_3	4.58	0.60	7.09
CaO	63.2	0.25	0.89
MgO	1.35	0.08	0.87
SO_3	1.29	0.78	4.28
LOI	1.3	7.35	4.01
Specific gravity	3.14	2.60	2.17
Specific surface area (m^2/kg)	302	2000	398

binding material for the entire experimental work. The physical properties and oxide composition of PC, MK, and PA is detailed in Table 1.

As per BIS: 3812–2013 [48], the chemical constituents of MK and PA predominantly consist of SiO_2, Al_2O_3, and Fe_2O_3, with their sum exceeding 70.0%, categorizing them as pozzolanic materials. The LOI values for MK and PA were determined to be 7.35 and 4.01, respectively. Manufactured sand (M-sand) and coarse aggregate (CA) were sourced from a local supplier, with M-sand serving as the fine aggregates and the CA being used for the research work, possessing a size of 20 mm. The properties of M-sand and CA can be found in Table 2. In addition, potable water was employed for both the mixing and curing processes in this investigative study.

2.2. Experimental program

This research work encompasses four types of concrete: control concrete (CC), binary blended metakaolin concrete (BBMC), binary blended pond ash concrete (BBPC), and ternary blended metakaolin and pond ash concrete (TBMPC). These concrete types were subjected to testing for slump and mechanical properties. In the case of CC, the mixture consisted solely of PC. BBMC mixtures were prepared with 4–20% of MK, BBPC mixes included 4–20% of PA, and TBMPC mixes integrated various proportions of both MK and PA. For this study, the concrete specimens were formulated using a mix composition of 1:1.75:2.22 at a water-cement ratio of 0.44. The specifics of the mix proportions are outlined in Table 3.

The concrete samples were cast and demolded after 24 hours of ambient curing, then immersed in water for 28 and 90 days before undergoing testing at the concrete lab. The study necessitated the evaluation of mechanical properties using a total of 288 specimens, as outlined in Table 4.

Table 2: Properties of the M-sand and coarse aggregate.

AGGREGATE	PROPERTIES			
	FINENESS MODULUS	SPECIFIC GRAVITY	ABSORPTION (%)	BULK DENSITY (kg/m^3)
M-sand	2.46	2.71	1	1850
Coarse aggregate	6.73	2.69	0.5	1695

Table 3: Mix proportion of CC, BBMC, BBPC and TBMPC.

MIX DETAIL	BINDER CONTENT (%)			W/B RATIO	MATERIALS (kg/m^3)					
	OPC	MK	PA		OPC	MK	PA	FA	CA	W
CC	100	0	0	0.44	448	0	0	788	996	197
MK_4	96	4	0		430.08	17.92	0			
MK_8	92	8	0		412.16	35.84	0			
MK_{12}	88	12	0		394.24	53.76	0			
MK_{16}	84	16	0		376.32	71.68	0			
MK_{20}	80	20	0		358.4	89.6	0			
PA_4	96	0	4		430.08	0	17.92			
PA_8	92	0	8		412.16	0	35.84			
PA_{12}	88	0	12		394.24	0	53.76			
PA_{16}	84	0	16		376.32	0	71.68			
PA_{20}	80	0	20		358.4	0	89.6			
MK_2PA_2	94	2	2		430.08	8.96	8.96			
MK_4PA_4	91	4	4		412.16	17.92	17.92			
MK_6PA_6	88	6	6		394.24	26.88	26.88			
MK_8PA_8	85	8	8		376.32	35.84	35.84			
$MK_{10}PA_{10}$	82	10	10		358.4	44.8	44.8			

Table 4: Details of the specimens.

MIX DETAIL	COMPRESSIVE STRENGTH (f_{cs})		SPLIT TENSILE STRENGTH (f_{sts})		FLEXURAL STRENGTH (f_{fs})		SUB TOTAL	TOTAL
	28 DAYS	90 DAYS	28 DAYS	90 DAYS	28 DAYS	90 DAYS		
CC	3	3	3	3	3	3	18	288
MK_4	3	3	3	3	3	3	18	
MK_8	3	3	3	3	3	3	18	
MK_{12}	3	3	3	3	3	3	18	
MK_{16}	3	3	3	3	3	3	18	
MK_{20}	3	3	3	3	3	3	18	
PA_4	3	3	3	3	3	3	18	
PA_8	3	3	3	3	3	3	18	
PA_{12}	3	3	3	3	3	3	18	
PA_{16}	3	3	3	3	3	3	18	
PA_{20}	3	3	3	3	3	3	18	
MK_2PA_2	3	3	3	3	3	3	18	
MK_4PA_4	3	3	3	3	3	3	18	
MK_6PA_6	3	3	3	3	3	3	18	
MK_8PA_8	3	3	3	3	3	3	18	
$MK_{10}PA_{10}$	3	3	3	3	3	3	18	

2.3. Test methods

2.3.1. Slump test

The fresh properties of the CC, BBMC, BBPC and TBMPC were assessed by means of a slump test. The test was performed immediately after the mixing process, as depicted in Figure 3a. The recorded slump value for all the mixtures were measured in millimeters (mm).

2.3.2. Mechanical properties

The mechanical properties of CC, BBMC, BBPC, and TBMPC were assessed in accordance with Indian regulations BIS 516–2004 [49], as detailed in Table 5.

f_{cs} test for CC, BBMC, BBPC, and TBMPC at 28 and 90 days was determined using a universal testing equipment with a 3000 kN capacity, as shown in Figure 3b. Likewise, f_{sts} test for these mixtures at 28 and 90 days was evaluated using the same 3000 kN capacity universal testing equipment, as shown in Figure 3c. Furthermore, the f_{fs} test for CC, BBMC, BBPC, and TBMPC were conducted at 28 and 90 days, employing a flexural testing equipment with a 100 kN capacity, as depicted in Figure 3d. The measured values for all mechanical properties of these mixtures were expressed in megapascals (MPa).

Figure 3: Experimental tests setup. (a) Slump test (b) f_{cs} test (c) f_{sts} test (d) f_{fs} test.

Table 5: The mechanical testing standards.

FRESH AND MECHANICAL PROPERTIES	DIMENSIONS	TESTING AGE	INDIAN STANDARDS CODE PROVISION
f_{cs} test	150 × 150 × 150 mm	28 and 90 days	BIS: 516-2004 [49]
f_{sts} test	150 × 300 mm (Φ × L)	28 and 90 days	
F_{fs} test	500 × 100 × 100 mm (L × B × D)	28 and 90 days	

3. RESULT AND DISCUSSION

3.1. Slump test

Figure 4 illustrates the slump value of BBMC mixes with 4–20% MK substituting for PC. The optimal slump, which is a measure of the mixtures fluidity, was observed to be 87 mm for the CC mix. However, for BBMC mixes with 20% of PC replaced by MK, the slump was significantly reduced to 41 mm. This decrease in slump can be attributed to the high reactivity and larger surface area of MK than PC. This perspective was associated with DHINAKARAN *et al.* [50], in which the workability of concrete declined as the percentage of PC replaced with MK increased. Similarly, TIWARI and BANDYOPADHYAY [51] observed that the finer texture of the pozzolan is crucial in maintaining the cohesiveness of the concrete mix and counteracting the decrease in workability as the MK content increases in the concrete. Similarly, the slump of BBPC mixes, with 4–20% of PC replaced with PA, is illustrated in Figure 4. The highest slump, measured at 87 mm, was seen in the CC mix, while the lowest slump was found to be 51 mm, occurring in the BBMPC with a combination of PA_{20} mix. This variation can be ascribed to the increased fineness of PA particles. This observation was linked to KHAN and GANESH [52], where the inclusion of PA and a gradual content increase of PA was associated with reduced concrete slump.

The alteration of the initial spherical particle shape due to grinding and the subsequent increase in fineness were the primary factors contributing to the decline in concrete workability [53]. Moreover, the workability of TBMPC mixtures, incorporating various percentages of MK and PA, is depicted in Figure 4. The highest slump, measured at 87 mm, was noted in the CC mix, whereas the lowest slump, recorded at 31 mm, occurred in the TBMPC with a combination of $MK_{10}PA_{10}$ mix. The findings suggest that the slump value of TBMPC diminishes with a higher proportion of MK and PA substituting for PC. This slump reduction can be traced back to the porous qualities of MK and PA particles, which, unlike PC, absorb more water as the MK and PA content in the mix rises. Similarly demonstrated a notable slump decrease as PC was replaced with MK, SCBA, and MHA in the mixture [54].

3.2. Compressive strength (f_{cs})

Figure 5 shows BBMC mixtures with different MK percentages replacing PC, assessing their f_{cs} at 28 and 90 days. The highest f_{cs}, 35.25 MPa at 28 days and 42.93 MPa at 90 days, was achieved with 12% of PC replaced by MK. In contrast, the lowest f_{cs}, 29.43 MPa at 28 days and 36.73 MPa at 90 days, was observed with 20% of MK used as a PC replacement material in concrete. It is evident that the f_{cs} is enhanced when using MK up to 12%, but further increases in MK content lead to a reduction in f_{cs}. This perspective is supported by MOGHADDAM *et al.* [55], where an increase in f_{cs} was noted with PC replacement by MK, up to 15%, at 28 days. Similarly, an enhancement in f_{cs} with a replacement of up to 10% of PC with MK in the mixture [56]. Figure 5 illustrates BBPC mixtures with varying proportions of PA used as a substitute for PC to assess their f_{cs} at both 28 and 90 days. The highest f_{cs}, reaching 34.15 MPa at 28 days and 41.52 MPa at 90 days, was achieved with 12% of PC replaced by PA.

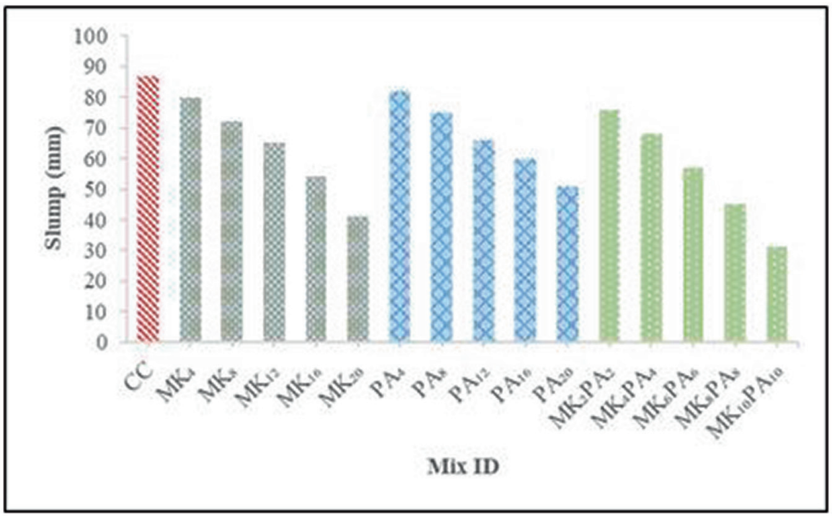

Figure 4: The slump value of CC, BBMC, BBPC and TBMPC mixes.

Figure 5: The f_{cs} of CC, BBMC, BBPC and TBMPC mixes.

Conversely, the lowest f_{cs}, measuring 28.82 MPa at 28 days and 35.47 MPa at 90 days, was observed in a mix with a 20% of PA. It's evident that the f_{cs} is enhanced when incorporating PA up to 12%, but further increases in PA content lead to a reduction in f_{cs}. This conclusion is supported by ARGIZ *et al.* [57], where an increase in f_{cs} was observed with the replacement of up to 10% of PC with PA, both at 28 and 90 days. Similarly, An enhancement in f_{cs} with the substitution of up to 10% of PC with PA in the mixture [58]. Moreover, Figure 5 depicts TBMPC mixtures, incorporating varying proportions of MK and PA, in order to evaluate their f_{cs} at both 28 and 90 days. The highest f_{cs}, measuring 36.23 MPa at 28 days and 43.63 MPa at 90 days, was achieved in the MK_6PA_6 mix, while the lowest f_{cs}, at 30.17 MPa for 28 days and 37.02 MPa for 90 days, was recorded in the $MK_{10}PA_{10}$ mix. It is evident that f_{cs} improve with the use of PC replacement in the MK_6PA_6 mixture, but subsequently declines. The enhancement in strength observed at 28 and 90 days can be attributed to the large proportions of silica content found in both MK and PA. These materials undergo a reaction with the excess portlandite, resulting in the formation of secondary C-S-H gel. This substance is known for its contribution to the increased strength of concrete. However, as more MK and PA are introduced into the concrete mixture, the strength starts to diminish. This decline is mainly attributed to MK and PA diluting the PC, leading to a decrease in available portlandite for secondary product. A similar approach was tested by BHEEL *et al.* [59], revealing an increase in f_{cs} when replacing PC with 10% of both MK and GGBS in the mixture at 28 days.

3.3. Splitting tensile strength (f_{sts}) and flexural strength (f_{fs})

Figures 6 and 7 illustrate BBMC mixtures with different MK percentages replacing PC, with a focus on evaluating their f_{sts} and f_{fs} at 28 and 90 days. The highest f_{sts} and f_{fs}, reaching 3.97 MPa and 5.44 MPa for 28 days, and 4.26 MPa and 5.78 MPa for 90 days, respectively, was achieved with 12% of PC replaced by MK. Conversely, the lowest strength, measuring 3.52 MPa for f_{sts} strength and 4.78 MPa for f_{fs} at 28 days, and 3.77 MPa for f_{sts} and 5.13 MPa for f_{fs} at 90 days, was observed in the mix with 20% MK. It is evident that both f_{sts} and f_{fs} improve when utilizing MK up to 12% as a PC replacement in the mixture, but with further additions of MK in concrete, both strengths start to decline. This viewpoint aligns with the findings of KHATIB and CLAY [60], where they observed an increase in f_{sts} and f_{fs} with PC replacement by MK, up to 10%, followed by a decrease after 28 days. The both f_{sts} and f_{fs} were enhanced when incorporating various dosages of MK as a pozzolan in concrete [61]. Similarly, Figures 6 and 7 depict BBPC mixtures with varying proportions of PA as a substitute for PC, focusing on evaluating their f_{sts} and f_{fs} at both 28 and 90 days. At 28 days, the highest f_{sts} and f_{fs}, reaching 3.94 MPa and 5.38 MPa, and at 90 days, 4.14 MPa and 5.72 MPa, were achieved with 12% of PA. In contrast, at 28 days, the lowest f_{sts} and f_{fs} was measured at 3.34 MPa and 4.83 MPa and at 90 days, the lowest f_{sts} and f_{fs} was assessed at 3.78 MPa and 5.06 Mpa with 20% of PA. It's noteworthy that the use of PA enhances both f_{sts} and f_{fs}, particularly up to 12%. Similarly, ARGIZ *et al.* [62] reported an improvement in both f_{sts} and f_{fs} with the substitution of up to 10% of PC with PA. Moreover, Figures 6 and 7 depicts TBMPC mixtures, incorporating varying proportions of MK and PA, in order to evaluate their f_{sts} and f_{fs} at both 28 and 90 days. MK_6PA_6 achieved the highest f_{sts} and f_{fs} at both 28 and 90 days, with values reaching 4.01 MPa and 5.52 MPa at 28 days, and 4.37 MPa and 5.88 MPa at 90 days. In contrast, $MK_{10}PA_{10}$ exhibited the lowest f_{sts} and f_{fs} values,

Figure 6: The f_{sts} of CC, BBMC, BBPC and TBMPC mixes.

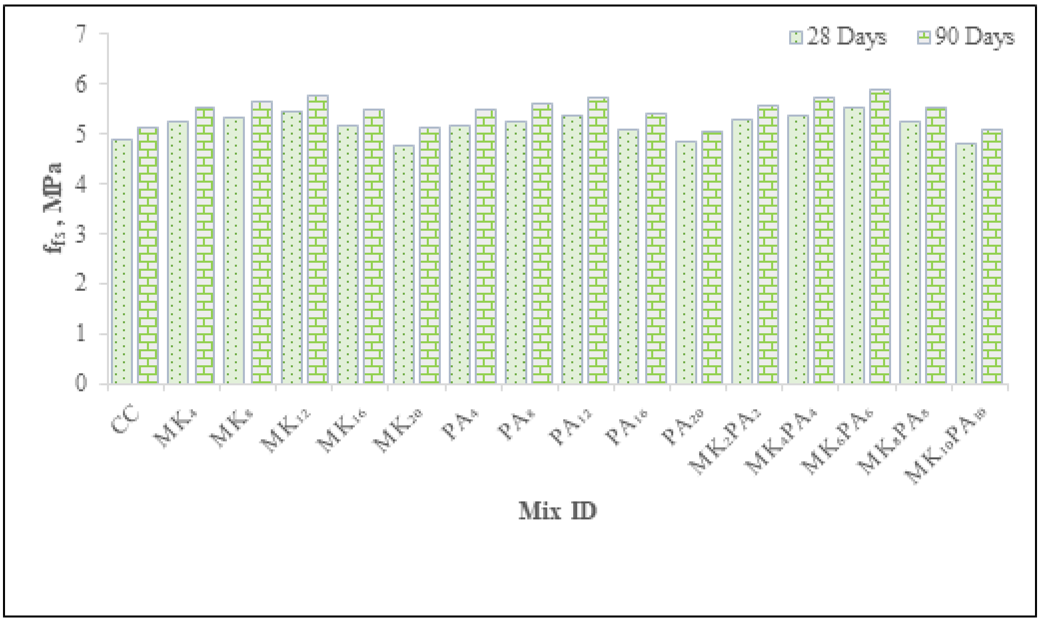

Figure 7: The f_{fs} of CC, BBMC, BBPC and TBMPC mixes.

measuring 3.48 MPa and 4.81 MPa at 28 days, and 3.76 MPa and 5.10 MPa at 90 days. It is evident that the f_{sts} and f_{fs} is enhanced with the use of PC replacement in the MK_6PA_6 mixture, but subsequently declines. The increase in strength observed at 28 and 90 days for BBMC, BBPC, and TBMPC can be attributed to the pozzolanic activity of MK and PA, which were quite similar, leading to the formation of an additional C-S-H gel. the reduction in strength can be attributed to the slower reaction of MK and PA than hydration of PC. This difference in reaction rates is due to the coarser particle sizes and higher levels of LOI in MK and PA than PC. This result aligns with TURKMEN and FINDIK [63], where using slag and metakaolin as PC replacements, up to 10%, enhanced concrete both f_{sts} and f_{fs}.

3.4. f_{cs} and f_{sts} relationship

A regression equation has been established to relate f_{cs} to f_{sts} of BBMC, BBPC and TBMPC at 28 days. This equation, derived through a power regression, is represented by equations. (1), (2) and (3), is visualized in Figure 8.

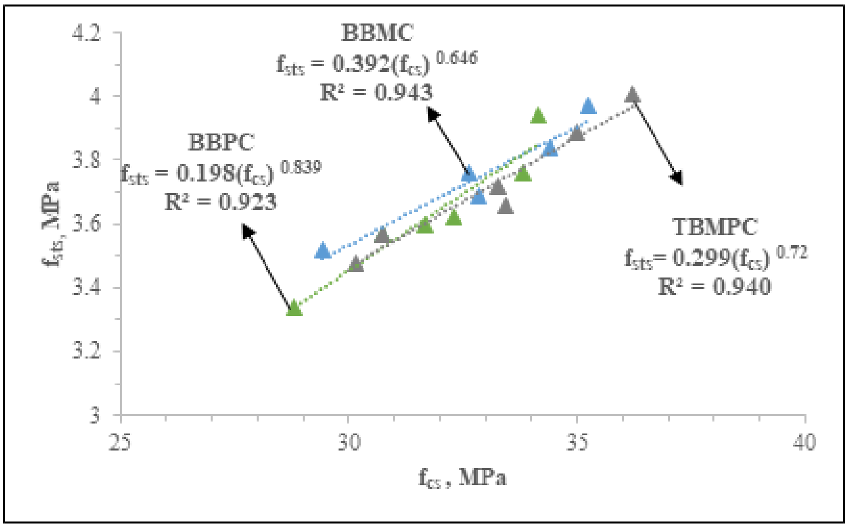

Figure 8: Relationship between f_{cs} and f_{sts} of BBMC, BBPC and TBMPC.

For BBMC

$$f_{sts} = 0.392(f_{cs})^{0.646}\ R^2 = 0.943 \quad (1)$$

For BBPC

$$f_{sts} = 0.198(f_{cs})^{0.839}\ R^2 = 0.923 \quad (2)$$

For TBMPC

$$f_{sts} = 0.299(f_{cs})^{0.720}\ R^2 = 0.940 \quad (3)$$

This association is consistent with the guidelines provided by ACI [64], NEVILLE [65], and CEB-FIP [66], which are detailed in equations (4), (5) and (6), correspondingly.

$$f_{sts} = 0.56(f_{cs})^{0.5} \quad (4)$$

$$f_{sts} = 0.23(f_{cs})^{0.67} \quad (5)$$

$$f_{sts} = 0.30(f_{cs})^{0.67} \quad (6)$$

Table 6 presents both the experimental and theoretical results of f_{sts}, derived from equations (4), (5) and (6).

For BBMC, BBPC, and TBMPC, the ratio between experimental and predicted f_{sts} values is close to 1, except for [65] equation (5). These findings are consistent with the earlier results [66].

3.5. f_{cs} and f_{fs} relationship

A regression equation has been formulated to establish a connection between the f_{cs} and f_{fs} of BBMC, BBPC, and TBMPC at the 28 days. This equation, derived via power regression, is delineated as equations (7), (8) and (9), and graphically represented in Figure 9.

For BBMC:

$$f_{fs} = 0.388(f_{cs})^{0.741}\ R^2 = 0.971 \quad (7)$$

For BBPC:

$$f_{fs} = 0.562(f_{cs})^{0.636}\ R^2 = 0.907 \quad (8)$$

Table 6: Comparison of experimental & theoretical f_{sts}.

MIX ID	EXPERIMENTAL f_{sts}		THEORETICAL f_{sts}, MPa			EXPERIMENT/THEORETICAL RATIO OF f_{sts}		
	FCS	FSTS	EQUATION (4)	EQUATION (5)	EQUATION (6)	EQUATION (4)	EQUATION (5)	EQUATION (6)
BBMC								
CC	30.75	3.57	3.10	2.28	2.97	1.15	1.57	1.20
MK_4	32.85	3.69	3.20	2.38	3.11	1.15	1.55	1.19
MK_8	34.42	3.84	3.28	2.46	3.21	1.17	1.56	1.20
MK_{12}	35.25	3.97	3.324	2.50	3.26	1.19	1.59	1.22
MK_{16}	32.64	3.76	3.20	2.37	3.09	1.18	1.59	1.22
MK_{20}	29.43	3.52	3.03	2.21	2.89	1.16	1.59	1.22
BBPC								
CC	30.75	3.57	3.10	2.28	2.97	1.15	1.57	1.20
PA_4	32.31	3.62	3.18	2.36	3.07	1.14	1.53	1.18
PA_8	33.82	3.76	3.25	2.43	3.17	1.16	1.55	1.19
PA_{12}	34.15	3.94	3.27	2.44	3.19	1.20	1.61	1.24
PA_{16}	31.65	3.6	3.15	2.32	3.03	1.14	1.55	1.19
PA_{20}	28.82	3.34	3.00	2.18	2.85	1.11	1.53	1.17
TBMPC								
CC	30.75	3.57	3.10	2.28	2.97	1.15	1.57	1.20
MK_2PA_2	33.26	3.72	3.22	2.40	3.13	1.16	1.55	1.19
MK_4PA_4	35.01	3.89	3.31	2.49	3.24	1.18	1.56	1.20
MK_6PA_6	36.23	4.01	3.37	2.54	3.32	1.19	1.58	1.21
MK_8PA_8	33.45	3.66	3.23	2.41	3.15	1.13	1.52	1.16
$MK_{10}PA_{10}$	30.17	3.48	3.07	2.25	2.94	1.13	1.55	1.18

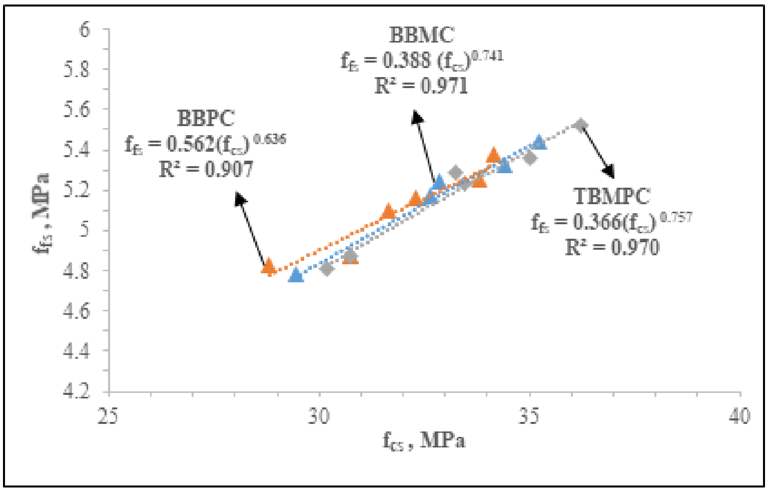

Figure 9: Relationship between f_{cs} and f_{fs} of BBMC, BBPC and TBMPC.

For TBMPC:

$$f_{fs} = 0.366(f_{cs})^{0.757} \quad R^2 = 0.970 \tag{9}$$

Equations (7), (8), and (9) outlines the connection between the f_{cs} and f_{fs} of BBMC, BBPC, and TBMPC. These equations are consistent with the standards set by JUKI *et al.* [67], LEGERON and PAULTRE [68], and BURG and OST [69], represented by equations (10), (11) and (12), respectively.

$$f_{fs} = 0.94\,(f_{cs})^{0.5} \tag{10}$$

$$f_{fs} = 0.517(f_{cs})^{0.5} \tag{11}$$

$$f_{fs} = 1.03(f_{cs})^{0.5} \tag{12}$$

Table 7 presents both the experimental and theoretical results of f_{fs}, derived from equations (10), (11) and (12).

In the case of BBMC, BBPC, and TBMPC, the ratio between experimental and predicted f_{fs} values is close to 1, with the exception of [68] equation (11). The R^2 values for these relationships align with those documented [69].

3.6. Sustainability analysis

In this research study, a sustainability analysis was conducted for sixteen mixtures to evaluate the carbon footprint of CC, BBMC, BBPC, and TBMPC, as detailed in Table 8. The data on carbon footprint emission for all concrete components were sourced from existing literature, with the exception of PA. Lack of data on PA carbon footprint in the literature has led to the reliance on a few assumptions in determining the carbon footprint. PA was obtained from a nearby thermal power plant in Mettur. It was transported to the testing laboratory, which was approximately 62 km away, using a 1000 kg-capacity diesel lorry truck. The emissions factor for this transportation was 0.192 $kgCO_2$/km. It is estimated that approximately 225 kWh of electricity will be needed to dry and sieve the 1000 kg of PA, as indicated by [75]. The emissions factor utilized is 0.521 $kgCO_2$ per kilowatt-hour, according to [76] one kg of PA is estimated to have a carbon footprint of 0.129 kg by using these emission factor values.

Figure 10 displays the carbon footprint of CC, BBMC, BBPC, and TBMPC. The carbon footprint of BBMC is as follows: 405 $kgCO_2/m^3$, 396 $kgCO_2/m^3$, 387 $kgCO_2/m^3$, 378 $kgCO_2/m^3$, and 369 $kgCO_2/m^3$.

Table 7: Comparison of experimental & theoretical f_{fs}.

MIX ID	EXPERIMENTAL f_{fs}		THEORETICAL f_{fs}, MPa			EXPERIMENT/THEORETICAL RATIO OF f_{fs}		
	f_{cs}	f_{fs}	EQUATION (10)	EQUATION (11)	EQUATION (12)	EQUATION (10)	EQUATION (11)	EQUATION (12)
BBMC								
CC	30.75	4.87	5.21	2.87	5.71	0.93	1.70	0.85
MK_4	32.85	5.24	5.38	2.96	5.90	0.97	1.77	0.89
MK_8	34.42	5.32	5.51	3.03	6.04	0.97	1.76	0.88
MK_{12}	35.25	5.44	5.58	3.07	6.12	0.97	1.77	0.89
MK_{16}	32.64	5.17	5.37	2.95	5.88	0.96	1.75	0.88
MK_{20}	29.43	4.78	5.10	2.80	5.59	0.94	1.71	0.86
BBPC								
CC	30.75	4.87	5.21	2.87	5.71	0.93	1.70	0.85
PA_4	32.31	5.16	5.34	2.94	5.85	0.97	1.76	0.88
PA_8	33.82	5.25	5.46	3.01	5.99	0.96	1.74	0.88
PA_{12}	34.15	5.38	5.49	3.02	6.02	0.98	1.78	0.89
PA_{16}	31.65	5.1	5.28	2.91	5.79	0.97	1.75	0.88
PA_{20}	28.82	4.83	5.04	2.78	5.53	0.96	1.74	0.87
TBMPC								
CC	30.75	4.87	5.21	2.87	5.71	0.93	1.70	0.85
MK_2PA_2	33.26	5.29	5.42	2.98	5.94	0.98	1.78	0.89
MK_4PA_4	35.01	5.36	5.56	3.06	6.09	0.96	1.75	0.88
MK_6PA_6	36.23	5.52	5.65	3.11	6.20	0.98	1.77	0.89
MK_8PA_8	33.45	5.23	5.43	2.99	5.96	0.96	1.75	0.88
$MK_{10}PA_{10}$	30.17	4.81	5.16	2.84	5.66	0.93	1.69	0.85

Table 8: Carbon footprint emissions for CC, BBMC, BBPC and TBMPC.

MIX DETAIL	PC	MK	PA	FA	CA	W	TOTAL CARBON FOOTPRINT EMISSIONS ($kgCO_2/m^3$)
	$kgCO_2$/kg/REFERENCES						
	0.82 [70]	**0.33 [71]**	**0.129 CURRENT STUDY ESTIMATE**	**0.0066 [72]**	**0.0408 [73]**	**0 [74]**	
CC	367	0	0	5	41	0	413
MK_4	353	6	0	5	41	0	405
MK_8	338	12	0	5	41	0	396
MK_{12}	323	18	0	5	41	0	387
MK_{16}	308	24	0	5	41	0	378
MK_{20}	294	29	0	5	41	0	369
PA_4	353	0	2	5	41	0	401
PA_8	338	0	5	5	41	0	389
PA_{12}	323	0	7	5	41	0	376
PA_{16}	308	0	9	5	41	0	363
PA_{20}	294	0	11	5	41	0	351
MK_2PA_2	353	3	1	5	41	0	403
MK_4PA_4	338	6	2	5	41	0	392
MK_6PA_6	323	9	3	5	41	0	381
MK_8PA_8	308	12	5	5	41	0	371
$MK_{10}PA_{10}$	294	15	8	5	41	0	363

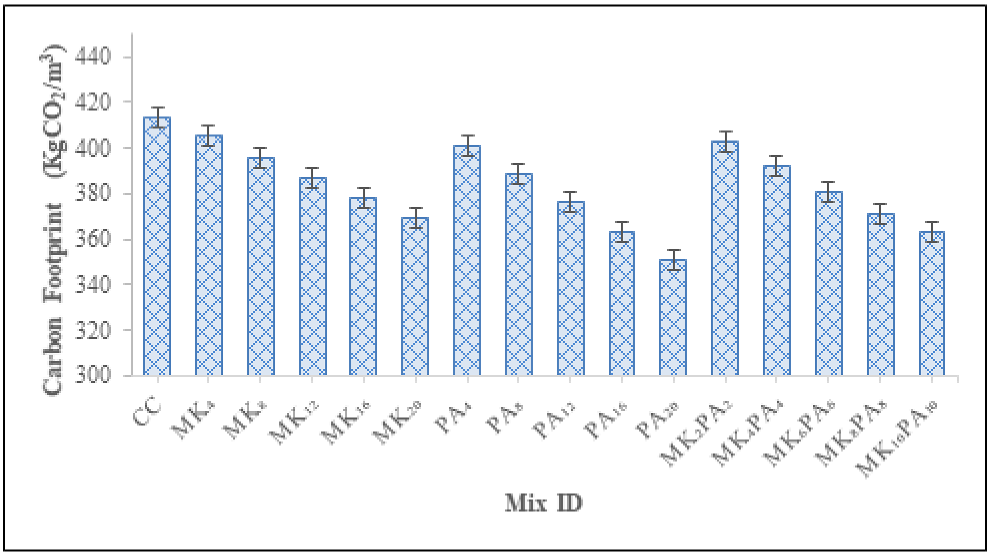

Figure 10: Carbon footprint of CC, BBMC, BBPC, and TBMPC.

These values are lower than that of the CC, which is 413 $kgCO_2/m^3$. However, the carbon footprint of BBPC is as follows: 401 $kgCO_2/m^3$, 389 $kgCO_2/m^3$, 376 $kgCO_2/m^3$, 363 $kgCO_2/m^3$, and 351 $kgCO_2/m^3$. These values are lower than that of the CC, which is 413 $kgCO_2/m^3$. Furthermore, the carbon footprint of TBMPC is as follows: 403 $kgCO_2/m^3$, 392 $kgCO_2/m^3$, 381 $kgCO_2/m^3$, 371 $kgCO_2/m^3$, and 363 $kgCO_2/m^3$. These values are also lower than that of the CC, which is 413 $kgCO_2/m^3$. The observations indicate that the reduction in carbon footprint is more pronounced in BBMC, BBPC, and TBMPC than control concrete.

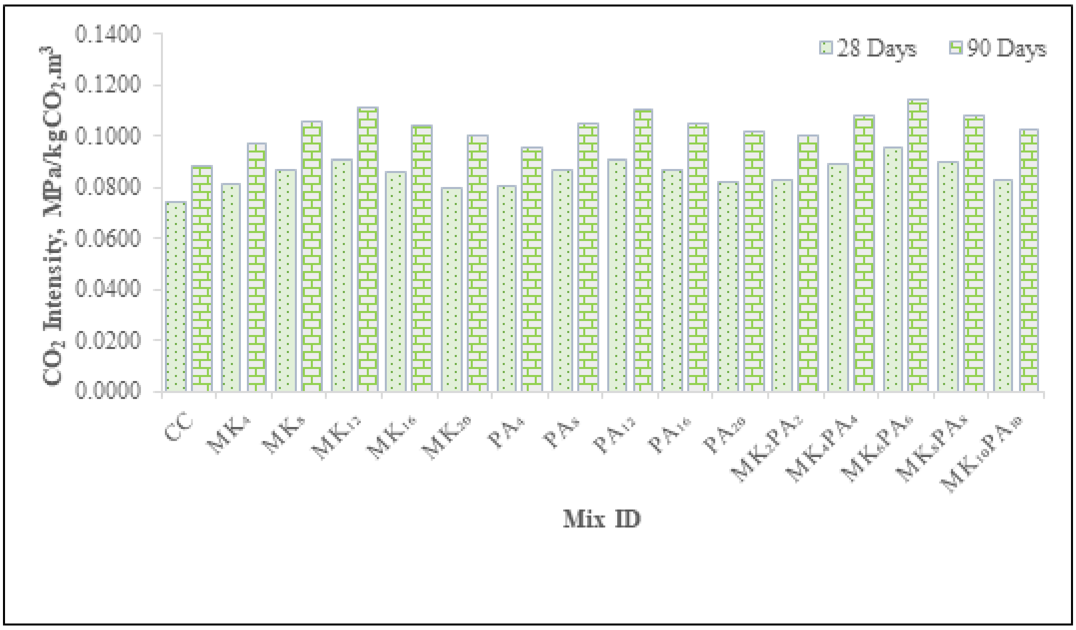

Figure 11: CO_2 intensity of CC, BBMC, BBPC, and TBMPC.

The sustainability analysis can also be evaluated with CO_2 intensity, calculated as the average 28-day f_{cs} of concrete divided by the total carbon footprint. The CO_2 intensity of BBMC, BBPC, and TBMPC was calculated and is depicted in Figure 11. At 28 days, the best CO_2 intensity was observed at 0.091 MPa/kgCO_2·m^3 for the 12% PC replaced with MK mix, 0.090 MPa/kg CO_2·m^3 for the 12% PA mix, and 0.095 MPa/kgCO_2·m^3 for the MK_6PA_6 mix. These values are higher than that of the CC mix (0.074 MPa/kgCO_2·m^3). At 90 days, the optimal CO_2 intensity was noted at 0.111 MPa/kgCO_2·m^3 for the 12% PC replaced with MK mix, 0.110 MPa/kgCO_2·m^3 for the 12% PA mix, and 0.114 MPa/kgCO_2·m^3 for the MK_6PA_6 mix. These values are also higher than that of the CC mix (0.088 MPa/kgCO_2·m^3). In a similar vein, at 28 days, the lowest CO_2 intensity was determined to be 0.079 MPa/kgCO_2·m^3 for the 20% MK mix, 0.082 MPa/kgCO_2·m^3 for the 20% PA mix, and 0.083 MPa/kgCO_2·m^3 for the $MK_{10}PA_{10}$ mix. Meanwhile, at 90 days, the lowest CO_2 intensity was calculated as 0.099 MPa/kgCO_2·m^3 for the 20% MK mix, 0.101 MPa/kgCO_2·m^3 for the 20% PA mix, and 0.102 MPa/kgCO_2·m^3 for the $MK_{10}PA_{10}$ mix. The observation suggests that the CO_2 intensity of BBMC, BBPC, and TBMPC improves as PC is replaced with MK and PA in concrete, up to 12%. However, with further additions, it begins to decrease.

4. CONCLUSIONS

The primary goal of this research endeavor is to investigate the impact and carbon footprint of BBMC, BBPC, and TBMPC mixtures. The experimental study led to the following conclusions:

1. The highest slump, measuring 87 mm, was observed for CC, while the lowest slump for BBMC and BBPC were 41 mm and 51 mm, respectively, at the MK_{20} and PA_{20} mix. Furthermore, the maximum slump was recorded at 87 mm for CC, and the minimum slump for TBMPC was 31 mm at the $MK_{10}PA_{10}$ mix.
2. The compressive strength values for CC were recorded at 30.75 MPa at 28 days and 36.61 MPa at 90 days. In the case of BBMC, at 28 days and 90 days, the Peak and lowest f_{cs} values were noted at 35.25 MPa and 29.43 MPa, 42.93 MPa and 36.73 MPa, with 12% of MK, and 20% of MK. For BBPC, at 28 days and 90 days, the Peak and lowest f_{cs} values were achieved at 34.15 MPa and 28.82 MPa, 41.52 MPa and 35.47 MPa, with 12% of PA, and 20% of PA. As for TBMPC, at 28 days and 90 days, the Peak and lowest f_{cs} values were attained at 36.23 MPa and 30.17 MPa, 43.63 MPa and 37.02 MPa, with MK_6PA_6 and $MK_{10}PA_{10}$ mixes. The findings indicate that the f_{cs} of BBMC, BBPC, and TBMPC improves when using PC replacement up to MK_{12}, PA_{12}, and MK_6PA_6 mixes. However, additional incorporations of these materials into concrete result in a strength decrease.
3. The f_{sts} values for CC were recorded at 3.57 MPa at 28 days and 3.85 MPa at 90 days. In the case of BBMC, at 28 days and 90 days, the highest and lowest f_{sts} values were measured at 3.97 MPa and 3.52 MPa, 4.26 MPa and 3.77 MPa, with 12% of MK, and 20% of MK. For BBPC, at 28 days and 90 days, the Peak and lowest

f_{sts} values were achieved at 3.94 MPa and 3.34 MPa, 4.14 MPa and 3.78 MPa, with 12% of PA, and 20% of PA. As for TBMPC, at 28 days and 90 days, the highest and lowest f_{sts} values were attained at 4.01 MPa and 3.48 MPa, 4.37 MPa and 3.76 MPa, with MK_6PA_6 and $MK_{10}PA_{10}$ mixes. The pattern suggests that f_{sts} of BBMC, BBPC, and TBMPC exhibits improvement when utilizing PC replacement up to 12% with MK, PA, and MK_6PA_6 mixes. However, incorporating these materials in higher proportions within the concrete results in a subsequent reduction in f_{sts}.

4. The f_{fs} values for CC were noted as 4.87 MPa at 28 days and 5.14 MPa at 90 days. Regarding BBMC, at 28 days and 90 days, the Peak and lowest f_{fs} values were measured at 5.44 MPa and 4.78 MPa, 5.78 MPa and 5.13 MPa, with 12% of MK, and 20% of MK. For BBPC, at 28 days and 90 days, the highest and lowest f_{fs} values were achieved at 5.38 MPa and 4.83 MPa, 5.72 MPa and 5.06 MPa, with 12% of PA, and 20% of PA. Similarly, for TBMPC, at 28 days and 90 days, the highest and lowest f_{fs} values were attained at 5.52 MPa and 4.81 MPa, 5.88 MPa and 5.10 MPa, with MK_6PA_6 and $MK_{10}PA_{10}$ mixes. The trend suggests that the f_{fs} of BBMC, BBPC, and TBMPC experiences improvement when utilizing PC replacement up to 12% with MK, PA, and MK_6PA_6 mixes. However, introducing these materials in higher proportions within the concrete subsequently leads to a reduction in f_{fs}.
5. The R^2 value suggests a strong correlation between f_{cs} and f_{sts}, as well as between f_{cs} and f_{fs}, in BBMC, BBPC, and TBMPC at 28 days.
6. The carbon footprint of BBMC, BBPA, and TBMPC decreased with increasing PC replacement by MK and PA, either separately or combined in concrete.
7. The experimental findings suggest that for BBMC, using 12% MK, for BBPC, using 12% PA, and for TBMPC, using MK_6PA_6 mix yields optimal results for construction purposes.

5. ACKNOWLEDGMENTS

The authors wish to acknowledge Department of Civil Engineering, K.S. Rangasamy College of Technology, Namakkal, Tamil Nadu for the facility and support extended for the research work.

6. BIBLIOGRAPHY

[1] UYSAL, M., AKYUNCU, V., “Durability performance of concrete incorporating Class F and Class C fly ashes”, *Construction & Building Materials*, v. 34, pp. 170–178, 2012. doi: http://dx.doi.org/10.1016/j.conbuildmat.2012.02.075.

[2] BAXI, J.M., *Monthly cement update*, https://www.jmbaxico.com/uploads/notifications/other/CEMENT March%20-%202023_jmbaxi.pdf?1680283415, accessed in December, 2023.

[3] NAQI, A., JANG, G.J., “Recent progress in green cement technology utilizing low-carbon emission fuels and raw materials: a review”, *Sustainability (Basel)*, v. 11, n. 2, pp. 537, 2019. doi: http://dx.doi.org/10.3390/su11020537.

[4] PURNELL, P., “The carbon footprint of reinforced concrete”, *Advances in Cement Research*, v. 25, n. 6, pp. 362–368, 2013. doi: http://dx.doi.org/10.1680/adcr.13.00013.

[5] SIVAKRISHNA, A., ADESINA, A., AWOYERA, P.O., et al., “Green concrete: A review of recent developments”, *Materials Today: Proceedings*, v. 27, pp. 54–58, 2019. doi: http://dx.doi.org/10.1016/j.matpr.2019.08.202.

[6] LAL MEGHWAR, S., WAHAB ABRO, A., ALI SHAR, I., et al., *Millet husk ash as environmental friendly material in cement concrete*, https://www.researchgate.net/publication/331859925, accessed in March, 2018.

[7] BATAYNEH, M., MARIE, I., ASI, I., “Use of selected waste materials in concrete mixes”, *Waste Management (New York, N.Y.)*, v. 27, n. 12, pp. 1870–1876, 2007. doi: http://dx.doi.org/10.1016/j.wasman.2006.07.026. PubMed PMID: 17084070.

[8] ADESINA, A., ATOYEBI, O.D., “Effect of crumb rubber aggregate on the performance of cementitious composites: a review”, In: *IOP Conference Series: Earth and Environmental Science*, v. 445, 2020. doi: http://dx.doi.org/10.1088/1755-1315/445/1/012032.

[9] CEVIK, A., ALZEEBAREE, R., HUMUR, G., et al., “Effect of nano-silica on the chemical durability and mechanical performance of fly ash based geopolymer concrete”, *Ceramics International*, v. 44, n. 11, pp. 12253–12264, 2018. doi: http://dx.doi.org/10.1016/j.ceramint.2018.04.009.

[10] GOLLAKOTA, A.R.K., VOLLI, V., SHU, C.M., “Progressive utilisation prospects of coal fly ash: a review”, *The Science of the Total Environment*, v. 672, pp. 951–989, 2019. doi: http://dx.doi.org/10.1016/j.scitotenv.2019.03.337. PubMed PMID: 30981170.

[11] SIDDIQUE, R., "Performance characteristics of high-volume Class F fly ash concrete", *Cement and Concrete Research*, v. 34, n. 3, pp. 487–493, 2004. doi: http://dx.doi.org/10.1016/j.cemconres.2003.09.002.

[12] BHEEL, N., ABBASI, S.A., AWOYERA, P., et al., "Fresh and hardened properties of concrete incorporating binary blend of metakaolin and ground granulated blast furnace slag as supplementary cementitious material", *Advances in Civil Engineering*, v. 2020, pp. 1–12, 2020. doi: http://dx.doi.org/10.1155/2020/8851030.

[13] BHEEL, N., AHMED, F., LAL, S., et al., "Millet husk ash as environmental friendly material in cement concrete millet husk ash as environmental friendly", *Materials and Cement Concrete*, v. 2018, pp. 153–158, 2019.

[14] ISLAM, M.M.U., MO, K.H., ALENGARAM, U.J., et al., "Mechanical and fresh properties of sustainable oil palm shell lightweight concrete incorporating palm oil fuel ash", *Journal of Cleaner Production*, v. 115, pp. 307–314, 2016. doi: http://dx.doi.org/10.1016/j.jclepro.2015.12.051.

[15] ALI SHAR, I., AYOUB, M.M., DAS BHEEL, N., et al., "Use of wheat straw ash as cement replacement material in the concrete", In: *International Conference on Sustainable Development in Civil Engineering*, Jamshoro, Pakistan, 2019. https://www.researchgate.net/publication/339434609, accessed in December, 2023.

[16] ALSALAMI, Z.H.A., HARITH, I.K., DHAHIR, M.K., "Utilization of dates palm kernel in high performance concrete", *Journal of Building Engineering*, v. 20, pp. 166–172, 2018. doi: http://dx.doi.org/10.1016/j.jobe.2018.07.015.

[17] RAJENDER, A., SAMANTA, A.K., "Compressive strength prediction of metakaolin based high-performance concrete with machine learning", *Materials Today: Proceedings*, 2023. In press. doi: http://dx.doi.org/10.1016/j.matpr.2023.03.522.

[18] KHATIB, J., *Sustainability of construction materials*, Amsterdam, Woodhead Publishing, 2016.

[19] ZELJKOVIC, M., "*Metakaolin effects on concrete durability*", M.Sc. Thesis, University of Toronto, Toronto.

[20] BASU, P.C., "High performance concrete", In *Proceedings INAE national seminar on engineered building materials and their performance*, pp. 426–450, 2003.

[21] KHATIB, J.M., "Metakaolin concrete at a low water to binder ratio", *Construction & Building Materials*, v. 22, n. 8, pp. 1691–1700, 2008. doi: http://dx.doi.org/10.1016/j.conbuildmat.2007.06.003.

[22] PATIL, B.B., KUMBHAR, P.D., "Strength and durability properties of high performance concrete incorporating high reactivity metakaolin", *Journal of Engineering Research*, v. 2, pp. 1099–1104, 2012.

[23] POON, C.S., LAM, L., KOU, S.C., et al., "Rate of pozzolanic reaction of metakaolin in high-performance cement pastes", *Cement and Concrete Research*, v. 31, n. 9, pp. 1301–1306, 2001. doi: http://dx.doi.org/10.1016/S0008-8846(01)00581-6.

[24] DINAKAR, P., SAHOO, P.K., SRIRAM, G., "Effect of metakaolin content on the properties of high strength concrete", *International Journal of Concrete Structures and Materials*, v. 7, n. 3, pp. 215–223, 2013. doi: http://dx.doi.org/10.1007/s40069-013-0045-0.

[25] EL-DIN, H.K.S., EISA, A.S., AZIZ, B.H.A., et al., "Mechanical performance of high strength concrete made from high volume of Metakaolin and hybrid fibers", *Construction & Building Materials*, v. 140, pp. 203–209, 2017. doi: http://dx.doi.org/10.1016/j.conbuildmat.2017.02.118.

[26] SALIMI, J., RAMEZANIANPOUR, A.M., MORADI, M.J., "Studying the effect of low reactivity metakaolin on free and restrained shrinkage of high performance concrete", *Journal of Building Engineering*, v. 28, pp. 101053, 2020. doi: http://dx.doi.org/10.1016/j.jobe.2019.101053.

[27] SHAFIQ, N., KUMAR, R., ZAHID, M., et al., "Effects of modified metakaolin using nano-silica on the mechanical properties and durability of concrete", *Materials (Basel)*, v. 12, n. 14, pp. 2291, 2019. doi: http://dx.doi.org/10.3390/ma12142291. PubMed PMID: 31319615.

[28] DINAKAR, P., "Design of self compacting concrete with fly ash", *Magazine of Concrete Research*, v. 64, n. 5, pp. 401–409, 2012. doi: http://dx.doi.org/10.1680/macr.10.00167.

[29] LAL, D., CHATTERJEE, A., DWIVEDI, A., "Investigation of properties of cement mortar incorporating pond ash—An environmental sustainable material", *Construction & Building Materials*, v. 209, pp. 20–31, 2019. http://dx.doi.org/10.1016/j.conbuildmat.2019.03.049.

[30] ARUMUGAM, K., ILANGOVAN, R., MANOHAR, D.J., "A study on characterization and use of pond ash as fine aggregate in concrete", *International Journal of Civil and Structural Engineering*, v. 2, pp. 466–474, 2011.

[31] DWIVEDI, A., LAL, D.K.S., "Influence of addition of pond ash as partial replacement with sand and cement on the properties of mortar", *International Journal of Innovative Technology and Exploring Engineering*, v. 2, n. 4, pp. 10–13, 2013.

[32] KUMAR, K.P., RADHAKRISHNA, X.X., "Workability strength and elastic properties of cement mortar with pond ash as fine aggregates", *Materials Today: Proceedings*, v. 24, n. Jun, pp. 1626–1633, 2020. doi: http://dx.doi.org/10.1016/j.matpr.2020.04.484.

[33] HAMMOND, G.P., JONES, C.I., "Embodied energy and carbon in construction materials", *Proceedings of Institution of Civil Engineers: Energy*, v. 161, n. 2, pp. 87–98, 2008. doi: http://dx.doi.org/10.1680/ener.2008.161.2.87.

[34] YUVARAJ, K., RAMESH, S., "A review on green concrete using low-calcium pond ash as supplementary cementitious material", *International Research Journal of Applied and Basic Sciences*, v. 26, n. 3, pp. 353–361, 2019. http://dx.doi.org/10.34256/irjmtcon47.

[35] YUVARAJ, K., RAMESH, S., "Experimental investigation on strength properties of concrete incorporating ground pond ash", *Cement, Wapno, Beton*, v. 3, n. 3, pp. 253–262, 2021. doi: http://dx.doi.org/10.32047/CWB.2021.26.3.7.

[36] TEMUUJIN, J., MINJIGMAA, A., BAYARZUL, U., et al., "Properties of geopolymer binders prepared from milled pond ash", *Materiales de Construcción*, v. 67, n. 328, pp. 1–11, 2017. doi: http://dx.doi.org/10.3989/mc.2017.07716.

[37] YUVARAJ, K., RAMESH, S., "Performance study on strength, morphological, and durability characteristics of coal pond ash concrete", *International Journal of Coal Preparation and Utilization*, v. 42, n. 8, pp. 2233–2247, 2022. doi: http://dx.doi.org/10.1080/19392699.2022.2101457.

[38] KURAMA, H., KAYA, M., "Usage of coal combustion bottom ash in concrete mixture", *Construction & Building Materials*, v. 22, n. 9, pp. 1922–1928, 2008. doi: http://dx.doi.org/10.1016/j.conbuildmat.2007.07.008.

[39] SUJJAVANICH, S., SUWANVITAYA, P., CHAYSUWAN, D., et al., "Synergistic effect of metakaolin and fly ash on properties of concrete", *Construction & Building Materials*, v. 155, pp. 830–837, 2017. doi: http://dx.doi.org/10.1016/j.conbuildmat.2017.08.072.

[40] AMBROISE, J., MAXIMILIEN, S., PERA, J., "Properties of metakaolin blended cements", *Advanced Cement Based Materials*, v. 1, n. 4, pp. 161–168, 2012. doi: http://dx.doi.org/10.1016/1065-7355(94)90007-8.

[41] KHAN, R., JABBAR, A., AHMAD, I., et al., "Reduction in environmental problems using rice-husk ash in concrete", *Construction & Building Materials*, v. 30, pp. 360–365, 2012. doi: http://dx.doi.org/10.1016/j.conbuildmat.2011.11.028.

[42] MOHD NASIR, N.A., MCCARTHY, M.J., "Effect of metakaolin on early strength of GGBS ternary concrete", *Applied Mechanics and Materials*, v. 584, pp. 1551–1557, 2014. doi: http://dx.doi.org/10.4028/www.scientific.net/AMM.584-586.1551.

[43] CHI, M.C., "Effects of sugar cane bagasse ash as a cement replacement on properties of mortars", *Science and Engineering of Composite Materials*, v. 19, n. 3, pp. 279–285, 2012. doi: http://dx.doi.org/10.1515/secm-2012-0014.

[44] BHAT, A.H., "Compressive strength and microstructural properties of sustainable concrete containing nanosilica, alccofine and metakaolin", *Civil Engineering Infrastructures Journal*, 2023. In press.

[45] SOUSA, M.I.C., RÊGO, J.H.S., "Effect of nanosilica/metakaolin ratio on the calcium alumina silicate hydrate (CASH) formed in ternary cement pastes", *Journal of Building Engineering*, v. 38, pp. 102226, 2021. doi: http://dx.doi.org/10.1016/j.jobe.2021.102226.

[46] YE, H., "Autogenous formation and smart behaviors of nitrite-and nitrate-intercalated layered double hydroxides (LDHs) in Portland cement-metakaolin-dolomite blends", *Cement and Concrete Research*, v. 139, pp. 106267, 2021. doi: http://dx.doi.org/10.1016/j.cemconres.2020.106267.

[47] BUREAU OF INDIAN STANDARDS, *IS: 12269-2013: Ordinary Portland Cement 53 Grade – Specification*, New Delhi, India, BIS, 2013.

[48] BUREAU OF INDIAN STANDARDS, *IS: 3812-2013: Indian standard pulverized fuel ash specification*, New Delhi, India, BIS, 2013.

[49] BUREAU OF INDIAN STANDARDS, *IS: 516-2004: Indian standard methods of tests for strength of concrete*, New Delhi, India, BIS, 2013.

[50] DHINAKARAN, G., THILGAVATHI, S., VENKATARAMANA, J., “Compressive strength and chloride resistance of metakaolin concrete”, *KSCE Journal of Civil Engineering*, v. 16, n. 7, pp. 1209–1217, 2012. doi: http://dx.doi.org/10.1007/s12205-012-1235-z.

[51] TIWARI, A.K., BANDYOPADHYAY, P., “Metakaolin for high performance concretes in India”, *Indian Concrete Journal*, v. 4, pp. 9–11, 2003.

[52] KHAN, R.A., GANESH, A., “The effect of coal bottom ash on mechanical and durability characteristics of concrete”, *Journal of Building and Material Structures*, v. 3, n. 1, pp. 31–42, 2016. doi: http://dx.doi.org/10.34118/jbms.v3i1.22.

[53] BURAK, F., SELCUK, T., HASAN, K., “Optimization of fineness to maximize the strength activity of high-calcium ground fly ash - Portland cement composites”, *Construction & Building Materials*, v. 3, n. 5, pp. 2053–2061, 2009. doi: http://dx.doi.org/10.1016/j.conbuildmat.2008.08.024.

[54] BHEEL, N., ALI, M.O., TAFSIROJJAMAN, N., et al., “Experimental study on fresh, mechanical properties and embodied carbon of concrete blended with sugarcane bagasse ash, metakaolin, and millet husk ash as ternary cementitious material”, *Environmental Science and Pollution Research International*, v. 29, n. 4, pp. 5224–5239, 2022. doi: http://dx.doi.org/10.1007/s11356-021-15954-4. PubMed PMID: 34417691.

[55] MOGHADDAM, F., SIRIVIVATNANON, V., VESSALAS, K., “The effect of fly ash fineness on heat of hydration, microstructure, flow and compressive strength of blended cement pastes”, *Case Studies in Construction Materials*, v. 10, pp. e00218, 2019. doi: http://dx.doi.org/10.1016/j.cscm.2019.e00218.

[56] KIM, H.S., LEE, S.H., MOON, H., “Strength properties and durability aspects of high strength concrete using Korean metakaolin”, *Construction & Building Materials*, v. 21, n. 6, pp. 1229–1237, 2007. doi: http://dx.doi.org/10.1016/j.conbuildmat.2006.05.007.

[57] ARGIZ, C., SANJUAN, M.A., MENENDEZ, E., “Coal bottom ash for Portland cement production”, *Advances in Materials Science and Engineering*, v. 17, pp. 1–7, 2017.

[58] JATURAPITAKKUL, R., CHEERAROT, T., “Development of bottom ash as pozzolanic material”, *Journal of Materials in Civil Engineering*, v. 15, n. 1, pp. 48–53, 2003. doi: http://dx.doi.org/10.1061/(ASCE)0899-1561(2003)15:1(48).

[59] BHEEL, N., MEMON, A.S., KHASKHELI, I.A., et al., “Effect of sugarcane bagasse ash and lime stone fines on the mechanical properties of concrete”, *Engineering, Technology & Applied Science Research*, v. 10, n. 2, pp. 5534–5537, 2020. doi: http://dx.doi.org/10.48084/etasr.3434.

[60] KHATIB, J.M., CLAY, R.M., “Absorption characteristics of metakaolin concrete”, *Cement and Concrete Research*, v. 34, n. 1, pp. 19–29, 2003. doi: http://dx.doi.org/10.1016/S0008-8846(03)00188-1.

[61] ARIKAN, M., SOBOLEV, K., ERTUN, T., et al., “Properties of blended cements with thermally activated kaolin”, *Construction & Building Materials*, v. 23, n. 1, pp. 62–70, 2009. doi: http://dx.doi.org/10.1016/j.conbuildmat.2008.02.008.

[62] ARGIZ, C., SANJUAN, M.A., MENENDEZ, E., “Coal bottom ash for portland cement production”, *Advances in Materials Science and Engineering*, v. 2017, pp. 6068286, 2017. doi: http://dx.doi.org/10.1155/2017/6068286.

[63] TURKMEN, I., FINDIK, S.B., “Several properties of mineral admixtures lightweight mortars at elevated temperatures”, *Fire and Materials*, v. 37, n. 5, pp. 337–349, 2013. doi: http://dx.doi.org/10.1002/fam.1030.

[64] AMERICAN CONCRETE INSTITUTE, *ACI 363-1999: State-of-the-art report on high strength concrete*, Michigan, ACI, 1999.

[65] NEVILLE, A.M., *Properties of concrete*, United Kingdom, Fourth and Final Edition, 1995.

[66] CEB-FIP, *Model code for concrete structures, evaluation of the time dependent behavior of concrete*, Bulletin CEB, 1990.

[67] JUKI, M.I., AWANG, M., MAHAMAD, M.K.A., et al., “Relationship between compressive, splitting tensile and flexural strength of concrete containing granulated waste polyethylene terephthalate (pet) bottles as fi ne aggregate”, *Advanced Materials Research*, v. 795, pp. 356–359, 2013. doi: http://dx.doi.org/10.4028/www.scientific.net/AMR.795.356.

[68] LEGERON, F., PAULTRE, P., “Prediction of modulus of rupture of concrete”, *ACI Materials Journal*, v. 97, n. 2, pp. 97, 2007.

[69] BURG, R.G., OST, B.W. “Engineering properties of commercially available high-strength concretes”, Portland Cement Association, Skokie, 1992.

[70] FLOWER, D.J.M., SANJAYAN, J.G., "Greenhouse gas emissions due to concrete manufacture", *The International Journal of Life Cycle Assessment*, v. 12, n. 5, pp. 282–288, 2007. doi: http://dx.doi.org/10.1065/lca2007.05.327.

[71] MEDDAH, M.S., ISMAIL, M.A., EL-GAMAL, S., et al., "Performances evaluation of binary concrete designed with silica fume and metakaolin", *Construction & Building Materials*, v. 166, pp. 400–412, 2018. doi: http://dx.doi.org/10.1016/j.conbuildmat.2018.01.138.

[72] CHEN, Y., FANG, Y., FENG, W., et al., "How to minimise the carbon emission of steel building products from a cradle-to-site perspective: a systematic review of recent global research", *Journal of Cleaner Production*, v. 21, pp. 133156, 2022. doi: http://dx.doi.org/10.1016/j.jclepro.2022.133156.

[73] TURNER, L.K., COLLINS, F.G., "Carbon dioxide equivalent (CO2-e) emissions: a comparison between geopolymer and OPC cement concrete", *Construction & Building Materials*, v. 43, pp. 125–130, 2013. doi: http://dx.doi.org/10.1016/j.conbuildmat.2013.01.023.

[74] JONES, R., MCCARTHY, M., NEWLANDS, M., "Fly ash route to low embodied CO2 and implications for concrete construction", In *World of Coal Ash (WOCA) Conference*, pp. 1–14, 2011.

[75] JHATIAL, A.A., GOH, W.I., MASTOI, A.K., et al., "Thermo-mechanical properties and sustainability analysis of newly developed eco-friendly structural foamed concrete by reusing palm oil fuel ash and eggshell powder as supplementary cementitious materials", *Environmental Science and Pollution Research International*, v. 28, n. 29, pp. 38947–38968, 2021. doi: http://dx.doi.org/10.1007/s11356-021-13435-2. PubMed PMID: 33745050.

[76] ALNAHHAL, M.F., ALENGARAM, U.J., JUMAAT, M.Z., et al., "Assessment on engineering properties and CO2 emissions of recycled aggregate concrete incorporating waste products as supplements to Portland cement", *Journal of Cleaner Production*, v. 203, pp. 822–835, 2018. doi: http://dx.doi.org/10.1016/j.jclepro.2018.08.292.